energy obtained for the $2s$ state is 0.2499 ry and for the $3p$ state 0.11110, as one would expect from the variational principle and the fact that (3.1) is exact for the $1s$ and $2p$ states. The $2s$ wave function cannot be exact if (3.1) is used for each shell, however, and the $3s$ energy can therefore be lower than the exact value; we find the value 0.1117 ry.

The wave functions are described by the parameters of Eq. (3.4), and these are listed in Table IV. The $3s$ wave function constructed in this way is compared with the corresponding hydrogen wave function in Fig. 4.

Similar results for hydrogen have been derived by Antončík[27] using the Thomas-Fermi expression (3.6) derived by Gombás.[20]

[27] E. Antončík, Czechoslov J. Phys. 7, 118 (1957).

PHYSICAL REVIEW VOLUME 116, NUMBER 2 OCTOBER 15, 1959

Magnetic Properties of the Manganese Chromite-Aluminates*

P. L. EDWARDS
United States Naval Ordnance Laboratory, White Oak, Maryland and University of Maryland, College Park, Maryland
(Received March 30, 1959)

The mixed-crystal spinel series $MnCr_{2-t}Al_tO_4$ has been synthesized and found to form a single cubic phase with a cell edge that is a linear function of the aluminum content. An x-ray study indicates that the series is an almost-normal spinel series with the A sites occupied by divalent manganese ions and about 5% of the trivalent aluminum ions.

The magnetization-temperature curves have approximately zero slope at absolute zero and exhibit no peaks or compensation points. The saturation moment is $1.16\mu_B$ for $t=0.0$, increasing to $1.37\mu_B$ at $t=0.8$, and dropping to $1.25\mu_B$ at $t=1.0$. The reciprocal-susceptibility *vs* temperature curves have the hyperbolic shape characteristic of ferrimagnets. The observed magnetic properties cannot be explained by the Néel theory but can be accounted for, at least qualitatively, by the five-parameter Yafet and Kittel theory.

INTRODUCTION

IN 1948 Néel showed that the magnetic moments of a number of magnetic oxides having the spinel structure and the chemical formula MN_2O_4 (where M is a divalent and N is a trivalent ion) can be explained in terms of two crystallographically unique sublattices A and B.[1] For the materials he considered, and many more studied since then, the interactions of the sublattices are such as to orient them antiparallel to each other, and the observed magnetic moment is the moment of one sublattice minus the moment of the other.

Although the Néel theory was very successful in many cases, there are theoretical objections to parts of the theory. For certain values of the interaction parameters, one of the two sublattices would be unsaturated, resulting in a nonzero slope of the magnetization *vs* temperature curve at absolute zero, which is in conflict with the third law of thermodynamics. Another objection is that for certain other values, which may be quite large, of the interaction parameters the material remains paramagnetic at all temperatures. This does not seem reasonable, since for strong interactions one would expect some kind of ordering at low temperatures.

Yafet and Kittel in 1952 published a modification of the Néel theory in which the two sublattices were again divided, giving four sublattices, A_1, A_2, B_1, and B_2, and which overcame the above difficulties.[2] Those cases explainable by the Néel theory are also explainable by this theory, and in a similar fashion. One feature of this theory is that for those cases in the Néel theory requiring an unsaturated A sublattice, for example, the Yafet and Kittel theory requires nonparallel alignment of saturated A_1 and A_2 sublattices. The Yafet and Kittel theory also introduced the interesting possibility that magnetic ordering transitions may occur at temperatures other than that at which the spontaneous moment appears.

The Yafet and Kittel theory has been used by several authors to explain observed magnetic effects that are not in agreement with the Néel model. Gorter has suggested that the saturation magnetization of the $MnCr_2O_4$-$MnFe_2O_4$ series might be explained in terms of angles on the B sublattice.[3] Lotgering has used the theory to explain the magnetization of $MnCr_2O_4$ and $FeCr_2O_4$ and has given approximate values of the interaction parameters.[4] The measurements of McGuire, Howard, and Smart[5] show a kink in the susceptibility curve of $NiCr_2O_4$ near 300°K, and later work by Volger[4] shows a specific heat anomaly and that by

* This paper is based on a thesis submitted to the Graduate School of the University of Maryland in partial fulfillment of the requirements for the degree of Doctor of Philosophy.

[1] L. Néel, Ann. phys. 3, 137 (1948).

[2] Y. Yafet and C. Kittel, Phys. Rev. 87, 290 (1952).

[3] E. W. Gorter, Philips Research Repts. 9, 295, 321, 403 (1954).

[4] F. K. Lotgering, Philips Research Repts. 11, 337 (1956).

[5] McGuire, Howard, and Smart, Ceram. Age 60, 22 (1952).

Braun[4] and Delorme[6] shows a crystallographic distortion there as well. These features are characteristic of an antiferromagnetic transition, which is one of the possible transitions of the Yafet and Kittel theory. The excess specific heat, however, is about one-half that expected for such a transition, and the distortion is greater than would be expected. Corliss and Hastings, using neutron diffraction techniques, have found a magnetic transition in $MnCr_2O_4$ at about 20°K, some 30° below the Curie temperature.[7] This might be a Yafet and Kittel transition. The neutron diffraction pattern, however, is quite complex and has not yet been completely analyzed. Prince has made a neutron diffraction study of $CuCr_2O_4$ from which he concludes that Yafet and Kittel angular arrangements occur in $CuCr_2O_4$.[8]

This paper reports on an experimental study of the magnetic properties of the spinel series $MnCr_2O_4$-$MnAl_2O_4$. This series was chosen for study because $MnCr_2O_4$ has a saturation moment at absolute zero which is inconsistent with the Néel theory and which had been attributed to Yafet and Kittel angles on the B sites by both Gorter and Lotgering. This is a particularly useful series for such a study because all members are approximately normal (within 5%, as will be shown). Thus all of the AA interactions are alike, as are all of the BB and all of the AB interactions. This is not the case in systems which have more than one type of magnetic ion on a sublattice. Thus it is apparent that this series represents the simplest case, at least theoretically, of a spinel with two nonidentical sublattices and two types of magnetic ions.

MATERIALS AND APPARATUS

Preparation of Materials

The generalized formula for the series is $MnCr_{(2-t)}Al_tO_4$. Samples were prepared from commercial certified chemicals for $t=0.00$, 0.20, 0.40, $\cdots$, 2.0. In order to prepare a sample, the correct proportions of $MnCO_3$, Cr_2O_3, and Al_2O_3 were weighed and mixed intimately for six hours in an alcohol slurry. The products were dried and then baked six hours at 1400°C in a helium atmosphere, after which the furnace power was turned off and the material cooled in the furnace, still with a helium atmosphere. Slow cooling had no observable effect on the properties of the samples. X-ray spectrometer patterns taken by using filtered Cr $K\alpha$ radiation at a scanning speed of $\frac{1}{4}$ degree per minute showed no lines other than those of the desired spinel.

Cation Distribution

Bertaut has shown that the 220/400 and 224/400 intensity ratios are very sensitive to the cation distribution in spinels but are relatively insensitive to the oxygen parameter.[9] The theoretical 220/400 ratios[10] are shown as lines in Fig. 1 for several values of γ, the fraction of the aluminum ions on the A sublattice. In order to calculate the theoretical ratios, atomic scattering factors were taken from *Internationale Tabellen, zur Bestimmung von Kristallstrukturen*, and the absorption edge corrections of Dauben and Templeton[11] were used. The oxygen parameter u was taken as 0.387. Wyckoff[12] gives $u=0.390$ for $MnAl_2O_4$, and by Romeijn's rule[13] concerning charge on A sites one obtains $u=0.387$ for $MnCr_2O_4$. The parameter u is a measure of the deviation of the oxygen ions from cubic close packing.

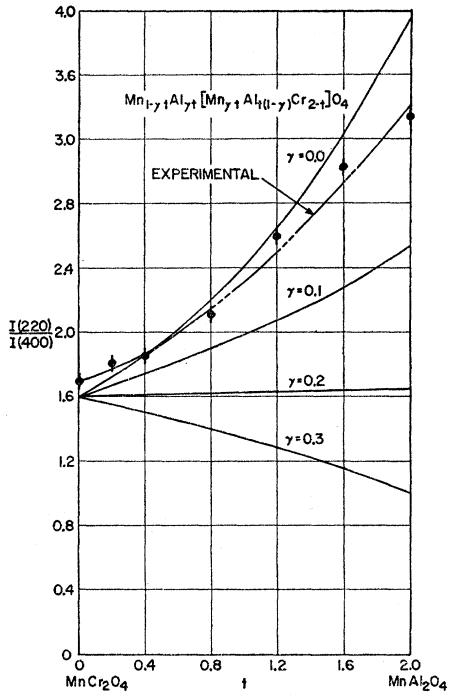

FIG. 1. Ratio of the intensity of the (220) to the (400) line as a function of aluminum content. γ is the fraction of aluminum ions on the A sites.

The experimentally determined ratios are shown as dots with vertical lines through them in Fig. 1. The vertical lines indicate the probable error due to the statistical nature of the x-ray beam.

[6] C. Delorme, Compt. rend. **240**, 1588 (1955).
[7] L. M. Corliss and J. M. Hastings (private communication).
[8] E. Prince, Acta Cryst. **10**, 554 (1957).
[9] F. Bertaut, Compt. rend. **230**, 213 (1950).
[10] The generalized chemical formula used for calculating the ratio is $Mn_{1-\gamma t}Al_{\gamma t}[Mn_{\gamma t}Al_{t(1-\gamma)}Cr_{2-t}]O_4$. In this formula the chromium ions are assumed to occupy B sites in all members of the series since these ions are known to have a strong preference for octahedral sites. No temperature factor was used in the intensity ratio calculations, and it is felt that the inclusion of the appropriate one, if known, would not make a significant difference in the results.
[11] C. H. Dauben and D. H. Templeton, Acta Cryst. **8**, 841 (1955).
[12] R. W. G. Wyckoff, *Crystal Structures* (Interscience Publishers, Inc., New York, 1951), Table VIII B, 2.
[13] F. C. Romeijn, Philips Research Repts. **8**, 304, 321 (1953).

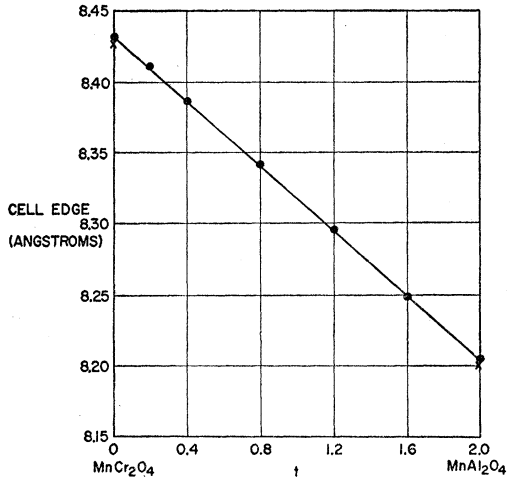

FIG. 2. Cell edge as a function of aluminum content. The crosses at $t=0$ and $t=2.0$ are Gorter's values.[3]

In Fig. 1 the theoretical lines for different values of γ converge to a point for $MnCr_2O_4$. This point corresponds to the theoretical ratio for the normal spinel $MnCr_2O_4$. From Corliss and Hastings[7] it is known that $MnCr_2O_4$ is normal; consequently, the theoretical and experimental points should coincide. That they do not must be attributed to a lack of knowledge concerning the true values of the atomic scattering factors. Therefore, it appears appropriate to shift the experimental curve downward until the theoretical and experimental points for $MnCr_2O_4$ coincide. When this is done, the data indicate that γ is relatively constant throughout the series and is probably less than 0.1.

Figure 2 shows the cell edge as a function of t. The series may be considered as a solid solution of manganese chromite and manganese aluminate. From the figure the cell edge is seen to vary linearly with t. This is in agreement with Vegard's law which states that "the lattice constants of solid solutions are linear functions of their compositions."[13] There is an additional point of interest here which holds for spinel solutions, however, since the cell edge of a spinel varies with its percentage normality. Thus, Vegard's law also implies that, for the case of a spinel solid solution where the cell edge varies linearly with composition, that the two components enter into solution with the same normality that they possess as pure materials. Now, since γ is equal to about 0.05 for manganese aluminate, Fig. 1, the linear cell edge variation implies that it has approximately this value throughout the series. This is in agreement with the results concerning γ obtained from the intensity ratio considerations and with the assumption that the chromium ions are on the B sites only. Thus the percentage normality of the series is given approximately as $100(1-0.05t)$ and the series is essentially a normal one.

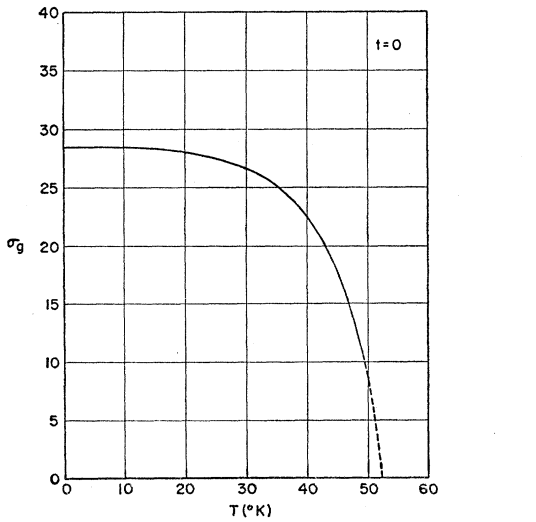

FIG. 3. Magnetization in cgs units per gram *versus* temperature for manganese chromite.

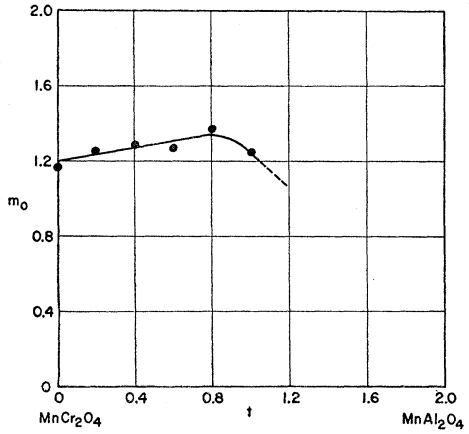

FIG. 4. Saturation moment m_0 in Bohr magnetons per formula unit at absolute zero for the series $MnCr_{2-t}Al_tO_4$.

Experimental Apparatus

The magnetic moments were determined by measuring the force on a sample in a nonuniform magnetic field. The force is given by

$$F_x=\sigma_g m(dH_x/dx), \qquad (1)$$

where σ_g is the magnetic moment per gram, m is the weight in grams, and dH_x/dx is the gradient of the field. By means of a glass rod the sample is hung from the arm of a chemical balance to the center of a short, thick solenoid which produces uniform magnetic fields of up to 15 000 oersteds. This is the field for magnetizing the sample. Located coaxially with the thick solenoid are two coils with fields opposed and so located that the resultant field is zero and the gradient is uniform at the sample position. Thus, with the weighed sample saturated by the solenoid field, the gradient field due to the gradient coils known, and the force on the sample determined using the balance, the saturation moment

can be calculated from Eq. (1). In order to make measurements down to liquid helium temperatures, it is necessary to locate the sample and balance in an air-tight enclosure with external controls and with provision for the evacuation of the enclosure and the introduction of a helium atmosphere. Temperatures from 4.2°K to room temperature were measured using a thermocouple of silver containing 0.37 atomic percent gold and gold containing 2.1 atomic percent cobalt.

EXPERIMENTAL RESULTS

The magnetization per gram σ_g as a function of temperature from 4.2°K to the Curie point was measured for values of t from 0.0 to 1.6. The curve σ_g-T for $t=0.0$ ($MnCr_2O_4$) at 6600 oersteds is shown in Fig. 3. The σ_g-T curves for other values of t are similar to the one shown. The initial slope of the magnetization curve

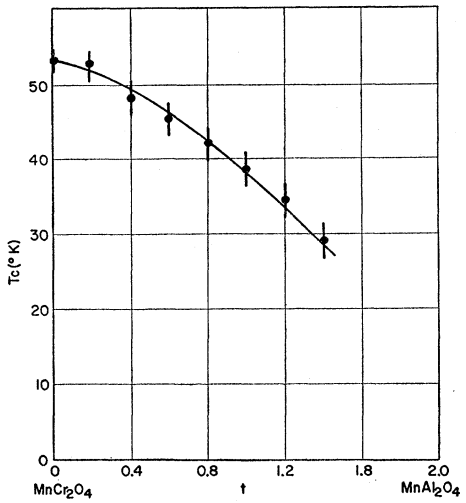

FIG. 5. Curie temperature as a function of aluminum content. The vertical lines indicate estimated uncertainty.

is approximately zero for all measured values of t, and there are no peaks or compensation points.

The Bohr magneton value is shown as a function of t in Fig. 4. The moment per formula unit is $1.16\mu_B$ for $t=0$ ($MnCr_2O_4$), rising to $1.37\mu_B$ at 0.8, and dropping to $1.25\mu_B$ at 1.0. For higher values of t the samples could not be saturated with the available fields so that it was not possible to determine the magneton values. It was evident, however, that the magneton values decreased toward zero as t approached 2.0.

The Curie temperature as a function of t is shown in Fig. 5. For $MnCr_2O_4$, the Curie temperature is 53°K. The Curie temperature decreases with increased aluminum substitution (higher values of t).

Figure 6 shows the reciprocal susceptibility as a function of temperature for $t=0.0$, 1.0, and 2.0 from the Curie temperature to room temperature. All curves have the hyperbolic shape characteristic of ferrimagnets.

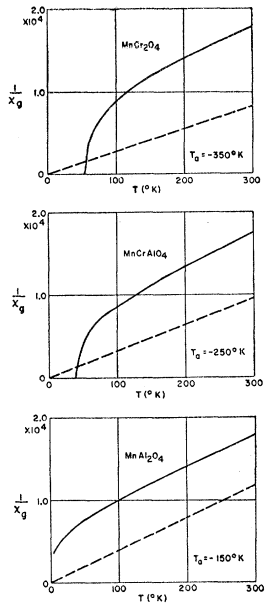

FIG. 6. Reciprocal susceptibility in cgs units per gram as a function of temperature for $MnCr_2O_4$, $MnCrAlO_4$, and $MnAl_2O_4$. The dashed lines indicate the theoretical high-temperature slope for spins of $\frac{5}{2}$ for divalent manganese and $\frac{3}{2}$ for trivalent chromium.

McGuire[14] has made microwave resonance measurements on $MnCr_2O_4$ and found $g_{\text{eff}}=2.1$.

COMPARISON WITH THEORY

Néel Theory

Néel's analysis predicted three possible ground states for a ferrimagnet, the state to be assumed depending on the relative values of the interaction parameters. These states are: (1) both sublattices saturated, (2) either the A or the B sublattice saturated and the other unsaturated, or (3) both sublattices paramagnetic. For state (1) the magnetic moment is a linear function of the aluminum substitution as indicated by Curve I in Fig. 7, which does not agree with the data at all. For state (2), the theory predicts a nonzero slope in the magnetization-temperature curves at absolute zero. For $MnCr_2O_4$ this slope would be about 35° on the curve of Fig. 3, which again is not in agreement with experiment. For state (3), the magnetic moment at absolute zero is zero, again in disagreement with the data. Thus the Néel theory does not explain the magnetic properties of this spinel series.

Yafet and Kittel Theory

The molecular fields acting on the sublattices A_1, A_2, B_1, and B_2 in the Yafet and Kittel theory are

$$\mathbf{h}_{Ai}=-n[(\alpha'-\alpha)\mathbf{a}_i+\alpha\mathbf{A}+\mathbf{B}], \quad i=1,2 \qquad (2)$$

$$\mathbf{h}_{Bi}=-n[\tfrac{1}{2}(\beta'-\beta)\mathbf{b}_i+\mathbf{A}+\beta\mathbf{B}], \quad i=1,2 \qquad (3)$$

where $\mathbf{a}_1$ is the magnetization of the A_1 sublattice, $\mathbf{b}_1$ is the magnetization of the B_1 sublattice, and $\mathbf{a}_1+\mathbf{a}_2=\mathbf{A}$ and $\mathbf{b}_1+\mathbf{b}_2=\mathbf{B}$. The five interaction parameters n, $n\alpha$,

[14] T. R. McGuire (private communication).

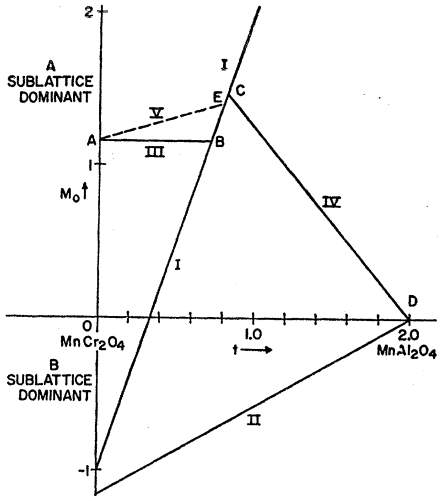

FIG. 7. Theoretical magnetic moments m_0 as a function of aluminum-substitution parameter t for different sublattice configurations. See text for discussion.

$n\alpha'$, $n\beta$, and $n\beta'$ are defined by the above equations. For a more complete consideration of the Yafet and Kittel theory see references 2, 3, and 4. The notation used here is based on that of Lotgering.[4]

An analysis of the interactions among the sublattices indicates that there are seven possible configurations of the sublattices. The possible configurations and the symbols used to represent them are: (1) $\mathbf{a}_1$ and $\mathbf{a}_2$ parallel, $\mathbf{b}_1$ and $\mathbf{b}_2$ parallel, and **A** and **B** antiparallel, $\uparrow\downarrow$, (2) $\mathbf{a}_1$ and $\mathbf{a}_2$ parallel, $\mathbf{b}_1$ at an angle (other than 0° or 180°) to $\mathbf{b}_2$, and **A** and **B** antiparallel, $|\rangle$, (3) $\mathbf{a}_1$ at an angle to $\mathbf{a}_2$, $\mathbf{b}_1$ and $\mathbf{b}_2$ parallel, **A** and **B** antiparallel, $\langle|$, (4) $\mathbf{a}_1$ and $\mathbf{a}_2$ antiparallel, $\mathbf{b}_1$ and $\mathbf{b}_2$ antiparallel, $\rightleftarrows\rightleftarrows$, (5) $\mathbf{a}_1$ and $\mathbf{a}_2$ antiparallel, B paramagnetic, $\rightleftarrows *$, (6) A paramagnetic, $\mathbf{b}_1$ and $\mathbf{b}_2$ antiparallel, $* \rightleftarrows$, and (7) A and B paramagnetic **. The particular configuration that the sublattices assume will depend on the sublattice magnetizations, the values of the interaction parameters, and through the magnetizations on the temperature.

In trying to fit the data to the theory, it is convenient to begin by considering the possible configurations of $MnCr_2O_4$ ($t=0$) at absolute zero ($T=0$). Since the spontaneous moment is finite, the configuration must be $\uparrow\downarrow$, $|\rangle$, or $\langle|$. The conclusions to be drawn from the theory concerning the magnetic properties of the series $MnCr_{2-t}Al_tO_4$ for the assumptions of $\uparrow\downarrow$, $|\rangle$, or $\langle|$ as the ground configuration of $MnCr_2O_4$ are presented here. It has been assumed that the interaction parameters, except as will be indicated, are constant. (Appendix Ia). The magnetic moment of the Cr^{+++} ion has been taken as $3\mu_B$ and of the Mn^{++} ion as $5\mu_B$.

Ground State $\uparrow\downarrow$ *for* $MnCr_2O_4$

If one assumes that the ground state for the whole series is $\uparrow\downarrow$, m_0 is given by Curve I of Fig. 7, which disagrees with the data. On the other hand, if one assumes that the ground state for $t=0$ ($MnCr_2O_4$) is $\uparrow\downarrow$, the theory leads to the prediction of the state $\langle|$ for higher t; that is, for increased aluminum substitution. This is essentially the same as the following case.

Ground State $\langle|$ *for* $MnCr_2O_4$

The magnetic moment in Bohr magnetons for this configuration is

$$m_0=4yS_B(1-1/\alpha), \tag{4}$$

where S_B is the spin for the Cr^{+++} ions, α is defined by Eq. (2), and $y=(2-t)/2$, the fraction of the B sublattice occupied by Cr^{+++} ions. Curve II of Fig. 7 is the moment as a function of t as predicted by Eq. (4) for constant α. A relatively smooth variation of α with t will bring Eq. (4) into agreement with experiment. A careful consideration of the magnetic data at $t=0$ and $t=1$ shows that it is not possible to describe the data with sets of parameters that are in reasonable agreement with each other. For example, α would have to change from 1.24 at $t=0$ to 1.73 at $t=1$, and $\beta+\frac{1}{3}\beta'$ from 0.69 to 0.04. Now, α and β are ratios of interaction parameters and therefore would not be expected to vary so much (Appendix Ib).

For the above molecular field parameters for $MnCr_2O_4$ the Eskowitz-Wangsness[15] formula for angular configurations gives $g_{\text{eff}}=1.85$, which is in poor agreement with the experimental value 2.1.

Ground State $|\rangle$ *for* $MnCr_2O_4$

The magnetic moment for this configuration is

$$m_0=2S_A(1-1/\beta), \tag{5}$$

where S_A is the spin of the Mn^{++} ions and β is defined by Eq. (3). Equation (5) shows that as long as the configuration $|\rangle$ exists m_0 is independent of the substitution parameter t. This configuration will exist for $\beta>a_0/yb_0$, where a_0 is the saturation moment for one-half mole of Mn^{++} ions and b_0 is that for one mole of Cr^{+++} ions. Given $m_0=1.16\mu_B$ and $S_A=\frac{5}{2}$ for $MnCr_2O_4$, β is 1.30 from Eq. (5). Using this value, the inequality is seen to hold up to $t=0.72$, Curve III of Fig. 7. For higher values of t, the configuration is $\uparrow\downarrow$ and the moment is given by Curve I of Fig. 7. This configuration exists for t up to values such that the inequality $\alpha>yb_0/a_0$ is satisfied, above which the moment is given by Eq. (4). The experimental moment at $t=1$ does not agree with that of Curve I; consequently, the latter inequality must hold. Substituting $m_0=-1.25\mu_B$, $y=\frac{1}{2}$, and $S_B=\frac{3}{2}$ into Eq. (4), we find that $\alpha=0.70$. The theoretically predicted moment for values of $t\geq 1$ is then given by Curve IV. It is thus seen that the predicted variation of m_0 with t based on the assumption that the ground state of $MnCr_2O_4$ is $|\rangle$ is given by the

[15] A. Eskowitz and R. K. Wangsness, Phys. Rev. **107**, 379 (1957).

curve $ABCD$ of Fig. 7. A better agreement with experiment is obtained if $\beta=1.30(1+0.07t)$, in which case the predicted moment is given by Curve $AECD$ of Fig. 7.

The above considerations bring the experimental m_0-t curve into line with the theory. This is only a part of the story, however. The theory, if correct, must explain not only the moment at absolute zero, but also the shapes of the magnetization and susceptibility curves as a function of temperature and of the substitution parameter t. The mathematical calculations to determine the five parameters that will do this reasonably well will not be considered here; a few of the more important considerations will be indicated, however. The experimental magnetization-temperature curves for the entire series were "normal" type curves with approximately zero slope at absolute zero, with no maxima as a function of temperature, and with no compensation temperatures. The experimental reciprocal-susceptibility curves have the characteristic hyperbolic shape of a ferrimagnet without any evidence of an antiferromagnetic transition. From the "normal" magnetization curves it is concluded that $\alpha\beta\approx 1$, which will be the case for $\alpha=0.77(1-0.07t)$. Taking into account the Curie temperature as a function of t and the absence of an observable antiferromagnetic transition in the susceptibility curves, it is possible to arrive at the following approximate values of the molecular field parameters:

t	α	α'	β	β'	n
0	0.77	0.20	1.30	0.18	50.4
1	0.70	0.30	1.40	−0.05	52.8

The variation of the parameters with t as indicated does not seem unreasonable in view of the change in cell edge shown in Fig. 2. The theoretical curves based on these parameters, together with the experimental data, are shown in Fig. 8 for $t=0$. The Eskowitz-Wangsness formula for g_{eff} gives 2.13 for $MnCr_2O_4$, in good agreement with the experimental value of 2.1.

DISCUSSION AND CONCLUSIONS

An antiparallel arrangement of saturated A and B sublattices cannot explain the observed magnetic moments at absolute zero for the manganese chromite-aluminate series. The x-ray evidence, together with Corliss and Hastings' neutron diffraction data on $MnCr_2O_4$, shows that the series is normal within 5%. The spins of $\frac{3}{2}$ for the trivalent chromium and $\frac{5}{2}$ for the divalent manganese are well established and are in agreement with the McGuire, Howard, and Smart's susceptibility data (asymptotic slope) on manganese chromite and with the susceptibility data reported here.

Although the Néel theory can explain the moments at absolute zero in terms of either unsaturated A or B sublattices, this explanation is ruled out by the zero slope of the magnetization curve at absolute zero.

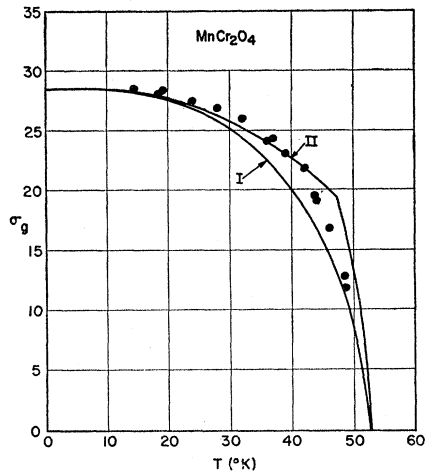

FIG. 8. Theoretical magnetization-temperature curves and data points for manganese chromite. Curve I is the Brillouin function for $s=\frac{3}{2}$ and is the theoretical curve for angles on the A sites at absolute zero. Curve II is the theoretical magnetization in cgs units per gram for angles on the B sites at absolute zero.

The Yafet and Kittel theory can explain the magnetic moments at absolute zero and the "normal" shape of the magnetization-temperature curves in terms of angles on the A sublattice or the B sublattice for manganese chromite; however, the assumption of angles on the B sublattice is preferred because it leads to a more reasonable variation of the molecular-field coefficients with aluminum substitution and to agreement between the theoretical and experimental g_{eff} for manganese chromite at liquid helium temperatures.

The reciprocal susceptibility-temperature curves have the characteristic shape predicted by the Néel theory. The absence of observable transition temperatures in these curves can be understood in terms of the Yafet and Kittel theory only if the transitions occur in the neighborhood of the Curie temperature so as to be obscured. This condition requires finite α' and β' so that a five-parameter Yafet and Kittel model is required rather than the three-parameter model assumed sufficient by Lotgering. The bending of the manganese-aluminate susceptibility curve towards the temperature axis is consistent with the spinel's being inverted a few percent as is indicated by the x-ray data.

The above considerations indicate that the observed data for the manganese chromite-aluminate series can be explained using the Yafet and Kittel theory assuming angles on the B sites for manganese chromite at absolute zero, finite α' and β' and reasonable variations of the molecular-field coefficients with the aluminum substitution.

ACKNOWLEDGMENTS

There are many in the Naval Ordnance Laboratory who have aided me in the course of this study, but I wish in particular to thank Dr. L. R. Maxwell, Dr. T. R. McGuire, Miss Selma Greenwald, and Dr. R. K.

Wangsness (also Professor of Physics (part-time) at the University of Maryland) for their assistance and support throughout this project.

APPENDIX I

The molecular field acting on the A_1 sublattice due to the B sublattice is $-n\mathbf{B}$, where n is the molecular field coefficient and $\mathbf{B}$ is the magnetization of the B sublattice. To a first approximation the Heisenberg theory gives, for nearest-neighbor interactions,

$$n=-2JZ/Ng^2\mu_B^2,$$

where J is the exchange integral, g is the Landé g factor, μ_B is the Bohr magneton, Z is the number of nearest neighbors that an A ion has on the B sublattice, and N is the number of ions on the B sublattice.[16]

a. If some nonmagnetic ions are substituted on the B sublattice so that the number of magnetic ions is yN, then the average number of magnetic nearest neighbors is yZ. Substituting these values for N and Z in the above equation shows that n does not change with the introduction of the nonmagnetic ions. This result also holds for the field coefficients $n\alpha$, $n\alpha'$, $n\beta$, and $n\beta'$, and can be shown to be independent of the assumption of nearest-neighbor interactions.

b. The substitution of aluminum for chromium may, however, influence the value of n through its effect on the exchange integral J, which in some cases is believed to be extremely sensitive to interatomic distances. These distances are decreased by the aluminum substitution, as indicated by Fig. 2. It might be expected, therefore, that the magnitude of J, and thus n, would be sensitive to the amount of aluminum substituted, but that α and β, being ratios of molecular field coefficients ($n\alpha/n$ and $n\beta/n$, respectively), would be relatively insensitive.

[16] J. H. Van Vleck, J. Chem. Phys. **9**, 85 (1941).

PHYSICAL REVIEW VOLUME 116, NUMBER 2 OCTOBER 15, 1959

High-Field Effect in Boron-Doped Silicon

R. D. LARRABEE
RCA Laboratories, Princeton, New Jersey
(Received May 18, 1959)

Two samples of boron-doped silicon were observed to have a linear current-voltage characteristic at liquid nitrogen temperature (77°K) up to fields of 10^4 volts/cm. This result was not expected since saturation of drift velocity is expected to occur at these high fields. Indeed, the current-voltage characteristic at 183°K did show the saturation effects expected. The experimental data seem to indicate that there is an appreciable amount (94%) of de-ionization of the boron level at 77°K and that the capture cross section of the ionized boron levels decreases as the hole drift velocity increases in the applied field. Since the thermal ionization rate is substantially independent of field, this implies that the steady-state number of carriers will be increased at the higher fields.

TWO samples of boron-doped silicon were observed to have a linear current-voltage characteristic at liquid nitrogen temperature (77°K) up to fields of 10^4 volts/cm. This result was not expected since saturation of drift velocity is expected to occur at these high fields. This paper describes some simple experiments which indicate that at low temperatures and high applied electric fields, several mechanisms may become operative that increase the number of majority carriers in the sample.

The resistivity *vs* temperature (for very low fields) of two boron-doped silicon samples is shown in Fig. 1. The initial decrease in resistivity as the temperature is decreased below room temperature is attributed to the increase in lattice mobility. It will be assumed that this power-law relationship of resistivity *vs* temperature would continue to be valid down to 77°K if it were not for the fact that at about 170°K one loses an appreciable number of carriers through de-ionization of the boron level. Consequently, from the extrapolated lattice mobility power-law relationship (straight lines of Fig. 1) and from the actual values of resistivity *vs* temperature observed, one can compute the amount of de-ionization as a function of temperature. The data so obtained are summarized in Fig. 2. Notice that the slope of the linear portion of this curve approximates the boron level (0.045 ev[1]) quite well. Consequently, it is reasonable to assume that this is the explanation of the curves of Figs. 1 and 2 and that the boron level is about 94% de-ionized at 77°K and substantially fully ionized above 170°K.

At 183°K one observes a reasonable current-voltage characteristic which shows signs of saturation at high fields. By assuming a doping of 9.5×10^{14} boron impurities/cm^3 for 15 ohm-cm material at room temperature[2] (for S640P), one can compute the drift velocity as a function of field from the current-voltage

[1] W. Kohn, in *Solid State Physics*, edited by F. Seitz and D. Turnbull (Academic Press, Inc., New York, 1957), Vol. 5, p. 258.
[2] M. B. Prince, Phys. Rev. **93**, 1204 (1954).